International Journal of Recent Technology and Engineering (IJRTE)
ISSN: 2277-3878 (Online), Volume-8 Issue-4, November 2019

Factors Affecting the Stability of Functionally Graded Sandwiched Beams

S.N.Padhi, K. S. Raghu Ram, Jasti Kasi Babu, K Suresh, T.Rout

Abstract: ***In this paper few of the factors affecting the dynamic stability of a steel-alumina functionally graded sandwiched (FGSW) beam have been discussed. The equation of motion was derived using both Hamilton's principle and finite element method. Floquet's theory was used to separate the stable zone from the unstable. The effect of hub radius parameter and rotational speed on first mode and second mode instability region of FGSW beam have been studied following the power law and exponential law. The results indicated that increasing hub radius and rotational speed keeps the instability region away from load factor axis and hence remote the chances instability of the beam.***

Index Terms: Exponential distribution, FGSW, load factor, Power law, Rotational speed, Hub radius, Stability.

I. INTRODUCTION

Composite materials have been playing an important role in the life of human beings since decades because of their ability to offer the desired properties.. Initially, bronze was frequently used which is actually an alloy of tin and copper. Bronze was first invented in 3700 BC, the era known as the Bronze Age [1]. Later on, a number of different alloys of metals and nonmetals were engineered for multiple purposes. The Metal Matrix Composites (MMCs) have been limited due to their higher cost and low fracture toughness as compared to metal alloys. Though MMCs are costly, they emerge as an important class of materials due to high specific strength and stiffness. Researchers found the utility of aluminium to be the second largest after steel. Aluminium and its metal matrix composite possess wide applications in various applications in aerospace industry, automobile industry, Constructions and even in kitchen utensils. Hybrid Al-MMC consist of two different materials, and one will be from organic origin along with the base material[2,9].The aluminium matrix is getting strengthened when it is reinforced with the hard ceramic particles like SiC, Al_2O_3 and B_4C etc. Aluminium alloys are still the subjects of intense studies, as their low density gives additional advantages in several applications.These alloys have started to replace cast iron and Bronze to manufacture wear resistance parts. MMCs reinforced with particles tend to offer enhancement of properties possessed by conventional routes[3,4]. As Glass fiber reinforced plastic (GFRP) composites possess high specific strength/stiffness, superior corrosion resistance, light weight, the GFRPs are widely used in engineering applications in the fields of aero industry, automobile applications and marine applications[5,7]. Epoxy resin can be produced with alkaline-treated fiber by hand-laying method. It also has been discovered that alkaline-treated composites with fiber load show outstanding tensile strength[6]. Coir fiber reinforced polymer resin composites with saturated ash particles is a new kind of promising composite material whose applications include Industrial Helmet, Dashboards of automobiles, Door panels, Light boards etc. Apart from these industrial applications some of the domestic applications are Decorative articles, Designer walls in hotels & malls , Welcome boards, etc [8].

The major disadvantage of composite materials is delamination at the interface. To overcome the drawback of conventional composite materials, a new breed of composite materials where the properties of the constituent materials required to be graded in space and further named as functionally graded materials (FGMs) which was first invented in 1984.

The research on functionally graded materials (FGMs) is rapidly growing because it can be a good replacement for the material of rotating beams. Timoshenko beam theory and classical Ritz method is employed to derive the governing equations. The equation of motion is derived using both Hamilton's principle and finite element method. Effects of various parameters such as rotating speeds, radius of hub and different functionally graded material properties on linear and nonlinear vibration characteristics are studied [10,13,15].

Recent investigations show that sandwich structures have much more advantages than the monolithic solid structure of the same materials and equal mass [11]. From a mechanics viewpoint, the main advantages of material property grading appear to be improving bonding strength, toughness, wear and corrosion resistance, and reduced residual and thermal stresses. The thermal stability of laminated functionally graded (FGM) circular plates of variable thickness subjected to uniform temperature rise is significantly influenced by the thickness variation profile, aspect ratio, the volume fraction index,

Manuscript published on November 30, 2019.
* Correspondence Author
Surya Narayan Padhi*, Dept.of Mechanical Engg., Koneru Lakshmaiah Education Foundation, Guntur, India.
K. S. Raghu Ram, **Jasti Kasi Babu,** Dept. of Mechanical Engg.,Vignan's Institute of Information Technology, Visakhapatnam, India.
K Suresh, Dept.of Mechanical Engg, GIT, GITAM.
Trilochan Rout, Dept.of Mechanical Engg., Parala Maharaja Engineering College, Berhampur,India

and the core-to-face sheet thickness ratio. plates with clamped edge are more resistant to buckling than plates with simply supported edge [12]. The FGM sandwich construction commonly exists in two types: FGM facesheet–homogeneous core and homogeneous facesheet–FGM core.

For the case of homogeneous core, the softcore is commonly employed because of the light weight and high bending stiffness in the structural design. The homogeneous hardcore is also employed in other fields such as control or in the thermal environments [14]. the geometrically nonlinear formulation based on von Karman's assumptions is employed to study the large amplitude free vibrations of functionally graded materials sandwich plates. The functionally graded material sandwich plate is made up of two layers of power-law functionally graded material face sheet and one layer of ceramic homogeneous core. A hierarchical finite element is employed to define the model, taking into account the effects of the transverse shear deformation and the rotatory inertia. The equations of motion for the nonlinear vibration of the functionally graded material sandwich plates are obtained using Lagrange's equations [16]. The study of effect of the system parameters on free vibration behavior of FGO and FGSW beams forms an important aspect of investigation [17]. A considerable amount of literature exists on sandwich panels as they are used in large number of applications varying from high-performance composites in aerospace structures to low-cost materials for building constructions. The limitations of classical plate theory in describing complex problems (e.g., contact/impact problems, behavior of thick laminate plates) necessitated the development of higher-order theories [18].

Many publications have been found on static and dynamic stability of ordinary beams. The literature on dynamic stability of functionally graded sandwiched rotating beams are found to be not in adequate number to the best of the authors' knowledge. The present article describes on the impact of radius of hub and rotation of a steel-alumina functionally graded sandwiched cantilever beam with on the dynamic stability of the beam.

II. FORMULATION

A functionally graded Timoshenko beam with alumina as top skin, steel as bottom skin is shown in Fig. 1(a). The beam is fixed at one end and free at the other end. A pulsating axial force $P(t) = P_s + P_t \cos \Omega t$, is applied on the beam and acting along its undeformed axis. P_s and P_t are respectively the static and dynamic components of the axial force, while Ω is the frequency of the dynamic component, and t is time. Fig. 1(a) shows the two noded finite element coordinate system used to derive the governing equations of motion.

Fig. 1(b) shows the expression for the displacements on (x-y) plane (reference plane) at the centre of the longitudinal axis. The thickness coordinate is measured as 'z' from the reference plane. The axial displacement and the transverse displacement of a point on the reference plane are, and respectively and is rotation of cross-sectional plane with respect to the un-deformed configuration. Figure 1(c) shows a two nodded beam finite element having three degrees of freedom per node.

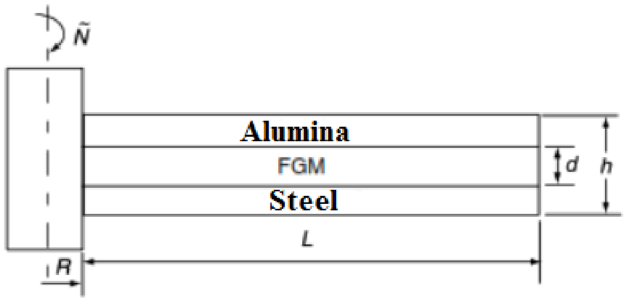

Figure 1(a) FGSW beam subjected to dynamic axial load.

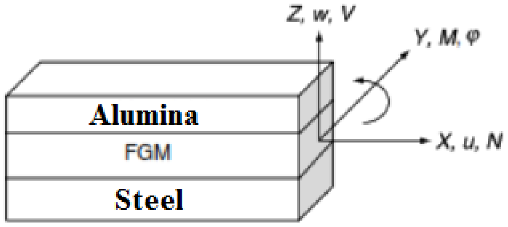

Figure 1(b) The coordinate system with generalized forces and displacements for the FGSW beam element.

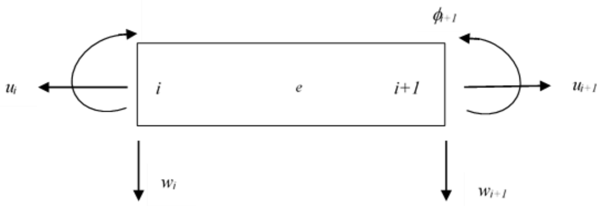

Figure 1(c) Beam element showing generalized degrees of freedom for ith element.

A. *Shape Functions*

According to the first order Timoshenko beam theory the displacement fields are expressed as

$$U(x,y,z,t) = u(x,t) - z\phi(x,t),$$
$$W(x,y,z,t) = w(x,t), \tag{1}$$

Where U = axial displacement and W = transverse displacement of a material point. The respective linear strains are

$$\varepsilon_{xx} = \frac{\partial u}{\partial x} - z\frac{\partial \phi}{\partial x}, \quad \gamma_{xz} = -\phi + \frac{\partial w}{\partial x} \tag{2}$$

The matrix form of stress-strain relation is

$$\{\sigma\} = \begin{Bmatrix} \sigma_{xx} \\ \tau_{xz} \end{Bmatrix} = \begin{bmatrix} E(z) & 0 \\ 0 & kG(z) \end{bmatrix} \begin{Bmatrix} \varepsilon_{xx} \\ \gamma_{xz} \end{Bmatrix} \tag{3}$$

Where $\sigma_{xx}, \tau_{xz}, E(z), G(z)$ and k are the normal stress on y-z plane, shear stress in x-z plane, Young's modulus, shear modulus and shear correction factor respectively. The variation of material properties along the thickness of the FGM beam governed by

(i) Exponential law is given by

$$M(z) = M_t \exp(-e(1-2z/h)) \tag{4}$$

$$e = \frac{1}{2}\log\left(\frac{M_t}{M_b}\right), \text{ and}$$

(ii) Power law is given by

$$M(z)=(M_t-M_b)\left(\frac{z}{h}+\frac{1}{2}\right)^n+M_b \qquad (5)$$

Where, $M(z)$ can be any one of the material properties such as, E, G and ρ etc., denote the values of The corresponding properties at top and bottommost layer of the beam are represented by M_t and M_b respectively, and the power index is n.

Now the shape function can be expressed as

$$\aleph(x)=\left[\aleph_u(x) \quad \aleph_w(x) \quad \aleph_\phi(x)\right]^T \qquad (6)$$

where, $\aleph_u(x)$, $\aleph_w(x)$, $\aleph_\phi(x)$ are the shape functions for the axial, transverse and rotational degree of freedom respectively.

B. Element Elastic Stiffness Matrix

The element elastic stiffness matrix is given by the relation

$$[k_e]\{\hat{u}\}=\{F\} \qquad (7)$$

where, $\{F\}$ = nodal load vector and $[k_e]$ = element elastic stiffness matrix.

C. Element Mass Matrix

The element mass matrix is given by

$$T=\frac{1}{2}\{\dot{\hat{u}}\}^T[m]\{\dot{\hat{u}}\} \qquad (8)$$

D. *Element Centrifugal* ***Stiffness Matrix***

The ith element of the beam is subjected to centrifugal force which can be expressed as

$$F_c=\int_{x_i}^{x_i+l}\int_{-h/2}^{h/2} b\rho(z)\tilde{N}^2(R+x)dzdx \qquad (9)$$

Where x_i = the distance between i[th] node and axis of rotation, $\tilde{N}$ and R are the angular velocity and radius of hub.

Work due to centrifugal force is

$$W_c=\frac{1}{2}\int_0^l F_c\left(\frac{dw}{dx}\right)^2dx=\frac{1}{2}\{\hat{u}\}[k_c]\{\hat{u}\} \qquad (10)$$

Where,

$$[k_c]=\int_0^l F_c[\aleph'_w]^T[\aleph'_w]dx \qquad (11)$$

E. Element Geometric Stiffness Matrix

The work done due to axial load P may be written as

$$W_p=\frac{1}{2}\int_0^l P\left(\frac{\partial w}{\partial x}\right)^2dx \qquad (12)$$

Substituting the value of w from eq. (6) into eq. (12) the work done can be expressed as

$$W_p=\frac{P}{2}\int_0^l\{\hat{u}\}^T[\aleph'_w]^T[\aleph'_w]\{\hat{u}\}dx$$

$$=\frac{P}{2}\{\hat{u}\}[k_g]\{\hat{u}\} \qquad (13)$$

here,

$$[k_g]=\int_0^l[\aleph'_w]^T[\aleph'_w]dx \qquad (14)$$

Where, $[k_g]$ = geometric stiffness matrix of the element.

III. EQUATION OF MOTION

Using Hamilton's principle.

$$\delta\int_{t_1}^{t_2}(T-S+W_p-W_c)dt=0 \qquad (15)$$

Substituting Eqns (7, 8, 10 and 13) into Eqn (15) and rewritten in Eqn (16)

$$[m]\{\ddot{\hat{u}}\}+\left[[k_{ef}]-P(t)[k_g]\right]\{\hat{u}\}=0 \qquad (16)$$

$$[m]\{\ddot{\hat{u}}\}+\left[[k_{ef}]-P^{\oplus}(\alpha+\beta_d\cos\Omega t)[k_g]\right]\{\hat{u}\}=0 \qquad (17)$$

$$[k_{ef}]=[k_e]+[k_c] \qquad (18)$$

where, $[k_e]$, $[k_c]$, $[m]$ and $[k_g]$ are elastic stiffness matrix, centrifugal stiffness matrix, mass matrix and geometric stiffness matrix respectively. $[k_{ef}]$ is the effective stiffness matrix. Assembling the element matrices as used in eq. (17), the equation of motion in global matrix form for the beam, can be expressed as

$$[M]\{\ddot{\hat{U}}\}+\left[[K_{ef}]-P^{\oplus}(\alpha+\beta_d\cos\Omega t)[K_g]\right]\{\hat{U}\}=0 \qquad (19)$$

Where $[M]$, $[K_{ef}]$, $[K_g]$ are global mass, effective stiffness and geometric stiffness matrices respectively and $[\hat{U}]$ is global displacement vector. Equation (19) represents a system of second order differential equations with periodic coefficients of the MathieuHill type. Floquet Theory has been used to distinguish between the dynamic stability and instability zones as follows. A solution with period 2T which is of practical importance is represented by

$$\hat{U}(t)=c_1\sin\frac{\Omega t}{2}+d_1\cos\frac{\Omega t}{2} \qquad (20)$$

Substituting eq. (20) into eq. (19) and solving the boundary solutions with period 2T. The resulting equation is given by

$$\left([K_{ef}]-(\alpha\pm\beta_d/2)P^{\oplus}[K_g]-\frac{\Omega^2}{4}[M]\right)\{\hat{U}\}=0 \qquad (21)$$

Equation (21) ends up with an eigenvalue problem with known quantities $P^{\oplus}$, α, β_d. Where $P^{\oplus}$ is the critical buckling load.

The plus and minus sign in the eq. (21) results with two sets of eigenvalues (Ω) binding the regions of instability and can be determined from the solution of the above equation

$$\left|[K_{ef}]-(\alpha\pm\beta_d/2)P^{\oplus}[K_g]-\frac{\Omega^2}{4}[M]\right|=0 \qquad (22)$$

A. Free Vibration

The eq. (22) can be written for a problem of free vibration by substituting α =0, β_d =0, and $\omega=\frac{\Omega}{2}$

$$\left|[K_{ef}]-\omega^2[M]\right|=0 \qquad (23)$$

The values of the natural frequencies $\{\omega\}$ can be obtained by solving eq. (23).

B. Static Stability

The eq. (22) can be written for a problem of static stability by substituting α =1, β_d =0, and $\omega=0$

$$\left|[K_{ef}]-P^{\oplus}[K_g]\right|=0 \qquad (24)$$

The values of buckling loads can be obtained by solving eq. (24).

C. Regions of Instability

ω_1 and $P^{\oplus}$ are calculated from eq. (23) and eq. (24) for an isotropic steel beam with identical geometry and end conditions ignoring the centrifugal force.

Choosing $\Omega=\left(\frac{\Omega}{\omega_1}\right)\omega_1$, eq. (22) can be rewritten as

$$\left|[K_{ef}]-(\alpha\pm\beta_d/2)P^{\oplus}[K_g]-\left(\frac{\Omega}{\omega_1}\right)^2\frac{\omega_1^2}{4}[M]\right|=0 \qquad (25)$$

For fixed values of α, β_d, $P^{\oplus}$, and ω_1, the eq. (25) can be solved for two sets of values of $\left(\frac{\Omega}{\omega_1}\right)$ and a plot between β_d and $\left(\frac{\Omega}{\omega_1}\right)$ can be drawn which will give the zone of dynamic instability.

IV. RESULTS AND DISCUSSION

A steel-alumina functionally graded sandwich (FGSW) rotating cantilever beam of length 1m and width 0.1m is considered for the parametric study. The bottom and top skin of the beam are steel and alumina respectively, whereas the core is the mixture of alumina and steel with bottom layer rich in steel. Both the top and bottom skin are of same thickness. The thickness of the core is 0.3 times of total thickness

The mechanical properties of the two phases of the beam are considered as given in the following table 1.

Table 1. Material properties of Steel-Alumina FGM beam.

Properties of steel	Properties of alumina
Young's modulus E =2.1x10^{11} Pa	Young's modulus E =3.9x10^{11} Pa
Shear modulus G =0.8x10^{11} Pa	Shear modulus G =1.37x10^{11} Pa
Mass density ρ =7.85x10^{3}kg/m^3	Mass density ρ =3.9x10^{3}kg/m^3
Poisson's ratio v is assumed as 0.3,shear correction factor k=(5+v)/(6+v)=0.8667	
Static load factor α =0.1	
Critical buckling load, $P^{\oplus}$ =6.49x10^7 N	
Fundamental natural frequency ω_1 =1253.1 rad/s	

The effect of hub radius parameter on the instability zone of FGSW-2.5 beam is investigated and presented in fig. 2(a) and 2(b) for first mode and second mode respectively. Figure 2(c) and 2(d) depict the plot of first and second mode instability regions of e-FGSW beam. Similar trends in the results are observed as in the case of FGO beam. Moreover, the effect is more prominent on FGSW beam as compared to that on FGO beams [15].

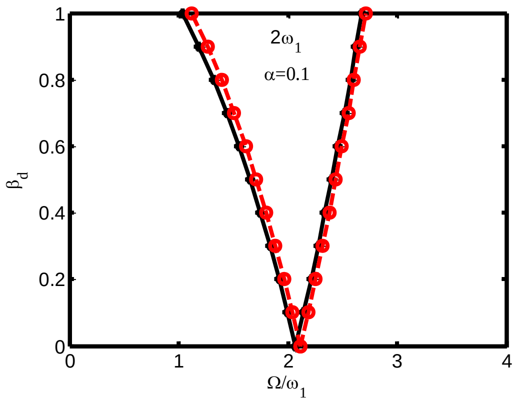

Figure 2(a). Effect of hub radius parameter on first mode instability region of steel-alumina FGSW-2.5 beam. S =0.2, V =1.15 ($^*\delta$ =0.1, ^{o} δ =0.5)

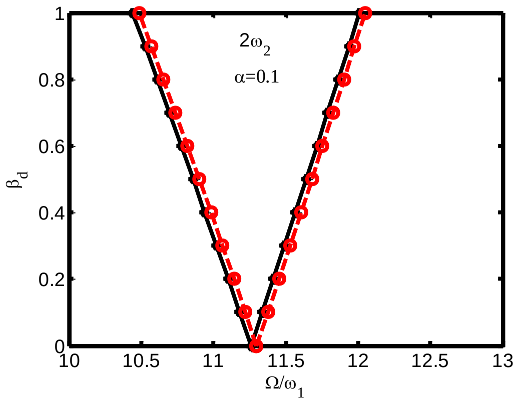

Figure 2(b). Effect of hub radius parameter on second mode instability region of steel-alumina FGSW-2.5 beam. S =0.2, V =1.15 ($^*\delta$ =0.1, ^{o} δ =0.5)

Retrieval Number: D4427118419/2019©BEIESP
DOI:10.35940/ijrte.D4427.118419
Journal Website: www.ijrte.org

Published By:
Blue Eyes Intelligence Engineering
& Sciences Publication

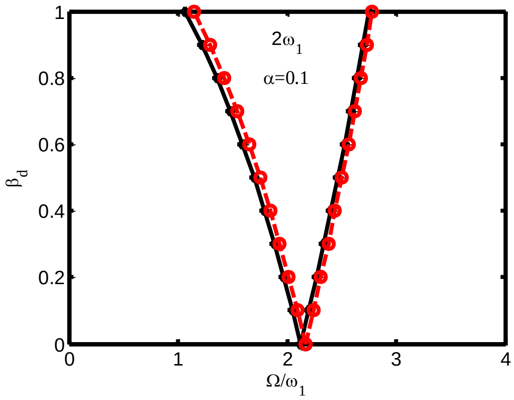

Figure 2(c). Effect of hub radius parameter on first mode instability region of steel-alumina e-FGSW beam. S =0.2, V =1.15 (*δ =0.1, o δ =0.5)

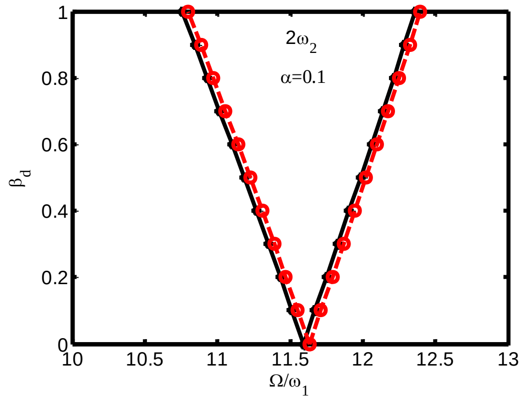

Figure 2(d). Effect of hub radius parameter on second mode instability region of steel-alumina e-FGSW beam. S =0.2, V =1.15 (*δ =0.1, o δ =0.5)

Figures 3(a) and 3(b) represent the effect of rotational speed on first and second mode instability zones of FGSW-2.5 beam and fig. 3(c) and 3(d) show the corresponding plots of e-FGSW beam. In all the cases it is found that increase in rotational speed enhances the stability of the beams, because the instability region corresponding to higher speed is situated away from the dynamic load factor axis and the area of instability region is decreased also.

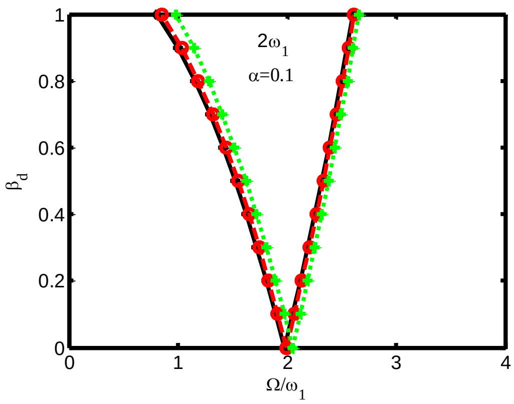

Figure 3(a). Effect of rotational speed parameter on first mode instability region of steel-alumina FGSW-2.5 beam. S =0.2, δ=0.1,d/h=0.3 (*ν =0.1, o ν =0.5, +ν=1.0)

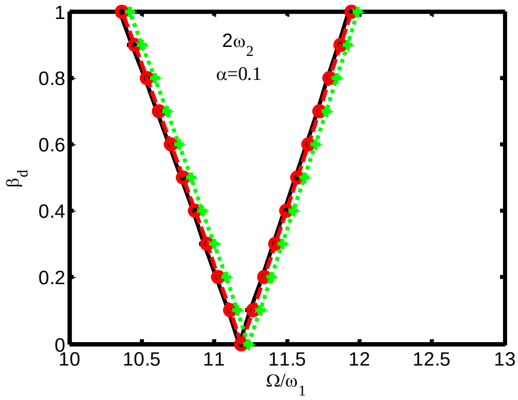

Figure 3(b). Effect of rotational speed parameter on second mode instability region of steel-alumina FGSW-2.5 beam. S =0.2, δ=0.1,d/h=0.3 (*ν =0.1, o ν =0.5, +ν=1.0)

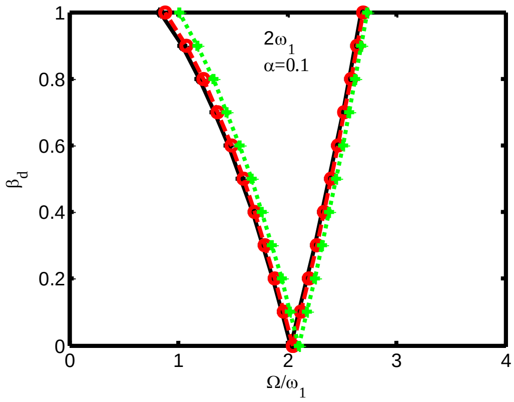

Figure 3(c) Effect of rotational speed parameter on first mode instability region of steel-alumina e-FGSW beam. S =0.2, δ=0.1,d/h=0.3 (*ν =0.1, o ν =0.5, +ν=1.0)

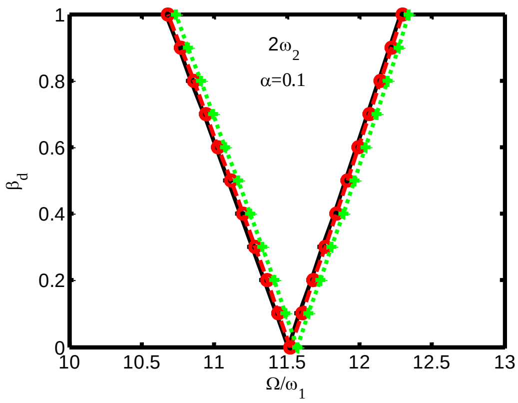

Figure 3(d). Effect of rotational speed parameter on second mode instability region of steel-alumina e-FGSW beam. S =0.2, δ=0.1,d/h=0.3 (*ν =0.1, o ν =0.5, +ν=1.0)

V.CONCLUSION

The dynamic stability analysis of FGSW rotating cantilever beams is investigated using finite element method. The material properties along the thickness of core of FGSW beam are assumed to follow either exponential law or power law. The effect of factors like rotational speed and hub radius on parametric instability of the beams is investigated.

Increase in rotational speed and hub radius of FGSW beams enhance their stability.

The increase of rotational speed increases the axial force in the beam, which in turn increases its stiffness. Therefore the dynamic stability is increased.

Exponential distribution of material properties ensures better dynamic stability compared to power law distribution of properties for FGSW beam.

It is evident from the above figures that the effect of hub radius and rotational speed parameter using power law and exponential law have similar result in first mode frequency. However exponential law ensures better stability in second mode frequency in both cases.

REFERENCES

1. The Bronze Age, February 2018 , http:// www.softschools.com/ timelines/the_bronze_age_timeline/145/.
2. Baburaja K., Teja Sainadh S., Sri Karthik D., Kuldeep J., Gowtham V., “Manufacturing and machining challenges of hybrid aluminium metal matix composites”, IOP Conference Series: Materials Science and Engineering, 2017, Vol.225(1), pp:1-9.
3. K. S. R. Ram, B. A. Ben, C. S. RamaKrishna and K. Monika, "Fracture toughness and mechanical properties of aluminum matrix composites with fly ash as reinforcement: An industrial waste recycling", International Conference on Electrical, Electronics, and Optimization Techniques (ICEEOT), Chennai, 2016, pp. 3859-3863.
4. K.S. Raghu Ram, Sharon Rose Sweanney Bandi and Ch. Sivarama Krishna, “ Mechanical Behaviour of Alumina Silicon Carbide Reinforced Particulate Reinforced Metal Matrix Composite”, IOP Conference Series: Materials Science and Engineering, Volume 225, 012181, pp:1-7.
5. K.S.Raghu Ram, Deepak P.D.S.N,Ch.Siva Rama Krishna and B.Avinash Ben, “Manufacturing and Delamination Study of Drilling on Glass Fiber Reinforced Plastic (GFRP)”, Australian Journal of Basic and Applied Sciences, 2015, Vol.9(36), pp: 391-395.
6. Mr. V. S. Jagadale, Dr. S. N. Padhi, “Mechanical Behavior of Coir Fiber Reinforced Epoxy Composites with Variable Fiber Lengths”, International Journal of Innovative Technology and Exploring Engineering, Volume-8 Issue-10, 2019.
7. Chintalapudi B.T., Gonuguntla C.B., Pothuri M., Kant J., Pathan A., Pittala R.K., “Investigation of mechanical properties of duralumin sandwich hybrid composite using E-glass fiber”, International Journal of Mechanical Engineering and Technology, 2017, Vol.8(5), pp:425-431.
8. Mr. V. S. Jagadale, Dr. S. N. Padhi, “Mechanical Behavior of Coir Fiber Reinforced Polymer Resin Composites with Saturated Ash Particles”, International Journal of Innovative Technology and Exploring Engineering, 2019, Vol.9(1),pp:3531-3535.
9. Baburaja K., Venkatasubbaiah K., Kalluri R., “Hybrid materials of aluminium”, Materials Today: Proceedings, 2016, Vol.3(10), pp:4140-4145.
10. S.N.Padhi, K.S.Raghuram, T.Rout, V.Naga Sudha, Gill Santosh Kumar, “Mechanical Property Variation of a Rotating Cantilever FGSW Beam under Parametric Excitation”, International Journal of Innovative Technology and Exploring Engineering,2019, Vol.8(11),pp:495-499.
11. Chunping Xiang, Qinghua Qin, Fangfang Wang, Mingshi Wang, Xuehui Yu, and T. J. Wang, “Large Deflection Response of Rectangular Metal Sandwich Plates with Functionally Graded Foam Core Subjected to Blast Loading”, 2016, Vol.725, pp:149-155.
12. S.K. Jalali, M.H. Naei, A. Poorsolhjouy, “Thermal stability analysis of circular functionally graded sandwich plates of variable thickness using pseudo-spectral method”, Materials & Design, 2010, Vol.31(10), pp:4755-4763.
13. S.N.Padhi, T.Rout, K.S.Raghuram, “Parametric instability and property variation analysis of a rotating cantilever FGO beam”, International Journal of Recent Technology and Engineering, 2019,Vol.8(1),pp:2921-2925.
14. Q. Li, V.P. Iu, K.P. Kou, “ Three-dimensional vibration analysis of functionally graded material sandwich plates”, Journal of Sound and Vibration, 2008, Vol.311(1-2), pp:498-515.
15. S.N.Padhi,G.Bhavani,V.Naga Sudha, K.S.Raghuram, T.Rout, “Effect of hub radius on rotational stability of functionally graded Timoshenko beams” , International Journal of Innovative Technology and Exploring Engineering,Vol.9(1), 2019 , pp:4246-4251.
16. Sid Ahmed Belalia, “Investigation of the mechanical properties on the large amplitude free vibrations of the functionally graded material sandwich plates”, Journal of Sandwich Structures & Materials, 2017, Vol.21(3), pp:895-916.
17. S.C. Mohanty, R.R. Dash and T. Rout, “Free Vibration of a Functionally Graded Rotating Timoshenko Beam Using FEM”, Advances in Structural Engineering, 2013, Vol.16(2), pp:405-418.
18. N.A. Apetre, B.V. Sankar, D.R. Ambur, “Analytical Modeling of Sandwich Beams with Functionally Graded Core”, Journal of Sandwich Structures & Materials, 2008, Vol.10(1), pp:53-74.